

INVESTIGATION OF THE STRUCTURE OF $\text{CaO-Al}_2\text{O}_3\text{-SiO}_2$ MELTS AS A BASIS FOR THE DEVELOPMENT OF NEW AGGLOMERATED WELDING FLUXES AND INDUSTRIAL REFRACTORIES

V.E. Sokol'skii^{a*}, D.V. Pruttskov^b, V.M. Busko^b, V.P. Kazimirov^a, O.S. Roik^a, A.D. Chyrkin^a,
V.I. Galinich^c, I.A. Goncharov^c

^a Taras Shevchenko National University of Kyiv, Kyiv, Ukraine

^b ZAO Tekhnokhim, Zaporozhye, Ukraine

^c E.O.Paton Electric Welding Institute

(Received 08 September 2017; accepted 29 June 2018)

Abstract

A significant number of welding fluxes and industrial ceramics are produced in the Ukraine. The production of these materials is sufficient for both domestic needs and significant export. It is assumed that the ternary $\text{CaO-Al}_2\text{O}_3\text{-SiO}_2$ system may become the basis for the development of agglomerated welding fluxes and technical ceramics. Three samples of ternary $\text{CaO-Al}_2\text{O}_3\text{-SiO}_2$ system were studied by means of high-temperature X-ray diffraction above the melting point: 23.3CaO-14.7Al₂O₃-62.0SiO₂ wt. % (sample 1, eutectic), 9.8CaO-19.8Al₂O₃-70.4SiO₂ wt. % (sample 2, eutectic), 15.6 CaO-36.5Al₂O₃-47.9SiO₂ wt. % (sample 3). Experimental scattering intensity curves, structure factors and the radial distribution function of atoms were obtained. The structural parameters of short-range order were calculated using melt structure models obtained by Reverse Monte Carlo method. The existence of microparticle associates of the mullite or sillimanite type immersed in the slag matrix is assumed. It is assumed that the calcium ions coordinated around these associates are surrounded by oxygen melt anions. Such a structure can be considered as a colloidal solution. The microparticle of mullite is the core of the aggregate that is surrounded by calcium and oxygen ions from the molten medium.

Keywords: Molten state; Heterogeneous region; Mullite; Eutectics; X-ray methods; Structure

1. Introduction

In the modern economic conditions the industry of the Ukraine needs to have cheap welding fluxes. Usually, in order to obtain fused fluxes, the remelting of the initial components with subsequent long exposure at high temperatures (1550-1800°C) is required. Therefore, the price of the fused fluxes has significantly increased recently, due to an increasing of the cost of the energy component in their production. Until now in Ukraine, the share of the fused welding fluxes in total production was more than 90 %. However, an increase in their price has caused the significant reduces of their competitiveness.

An alternative to the fused fluxes is an application of agglomerated (ceramic) fluxes for welding and surfacing. These fluxes are obtained by mixing raw materials, their granulation using liquid glass and subsequent low-temperature annealing at 500 -800° C. It should be noted that applying of this technology significantly reduces their price in comparison to fused fluxes.

The composition of agglomerated fluxes

traditionally differs from their fused analogs, which can be used for the same purposes. It is due to the fact that not all of the components of the agglomerated flux manage to melt and form an efficiently interacting medium with the molten metal during fast welding process.

This is due to the fact that the non-melted crystalline components in agglomerated flux interact weakly with the metal melt to be welded. On the other hand, quenched amorphous fused fluxes retain the structure of the initial melt and show good interaction with the metal melt, with the participation of all its components. Therefore, the development of new ceramic fluxes and improvement of existing ones is an actual task of modern material science. The X-ray diffraction and SEM/EDX (Scanning Electron Microscopy with Energy Dispersive X-Ray Analysis) studies of a model ceramic flux of the composition MgO (10% wt) -Al₂O₃ (25.5 wt) -SiO₂ (40% wt) -CaF₂ (25% wt) [1], which are successfully used for welding and surfacing of various steels, have shown that after annealing at 1500°C a complex oxide compound CaAl₂Si₂O₈ (anorthite) is formed. It means that part of the calcium fluoride (due to the transition of a portion

*Corresponding author: sokol@univ.kiev.ua



of MgO to MgF₂) is converted to an oxide form.

The CaO-Al₂O₃-SiO₂ oxide system is one of the most important slag compositions. Such slag is used in blast-furnace cast process as welding fluxes, etc. The ternary (anorthite, helenite) and binary (mullite) oxide compounds are formed in the system of CaO-Al₂O₃-SiO₂. The investigation of the structure of this melts has considerable scientific interest. This ternary oxide system has an extreme importance for metallurgical industry and materials science. Therefore, it is quite logical to obtain detailed information about interactions in the ternary CaO-Al₂O₃-SiO₂ system and more complex systems on its base. Some information about the properties and the structure of this system can be obtained from [2-5]. It should be noted that the CaO-Al₂O₃-SiO₂ system is also very important as a basis for obtaining many refractory materials and technical ceramics.

The increasing of productivity of process of submerged arc welding is connected with rising of the welding process speed. It can be achieved by a significant increase in the temperature of the weld pool and the power consumption. However, welding slags can not provide fast welding process due to low viscosity (spreading, rupture of the protective film, etc.). A flux based on the system CaO-Al₂O₃-MgO is under development [5]. Preliminary investigations of melted slags pointed out that it consists of melt and spinel particles. This spinel exists up to 2000°C. The formation of the spinel at high temperatures in melted samples of the CaO-Al₂O₃-MgO system is the cause of its high viscosity. Similar formation of microparticles at high-temperatures can take place in the CaO-Al₂O₃-SiO₂ melts. Therefore, the high-temperature studies of the structure and phase content of CaO-Al₂O₃-SiO₂ melts are very important to obtain welding fluxes with high viscosity. The obtained data on this system in the field of refractories will allow reducing the prime cost, due to the determination of the optimum annealing temperatures and its time.

The main purpose of this work is to create a scientific base for the development of ceramic welding fluxes, refractories, and technical ceramics, based on the ternary system CaO-Al₂O₃-SiO₂. Three samples (Table 1) were selected for structural analysis using the X-ray diffraction technique. Two selected compositions of samples 1 and 2 are triple eutectics and sample 3 is a nonvariant point [6]. In the future, it is planned to investigate other compositions and more complex systems on its base

2. Experimental procedure

The samples were prepared from high purity powders of Al₂O₃, SiO₂ and CaCO₃. The powder mixtures were annealed in the Tamman furnace for 1 h at 1873 K in the flow of high purity argon with further

Table 1. Composition, melting points, test temperatures and phase composition of studied samples

№	Composition, mass%			Melting temperature, K [6]	Temperature of the experiment, K	Phase composition
	CaO	Al ₂ O ₃	SiO ₂			
1	23.3	14.7	62	1443	298, 1573, 1623, 1673, 1723, 1743	CaAl ₂ Si ₂ O ₈ , CaSiO ₃ , SiO ₂
2	9.8	19.8	70.4	1618	298, 1673, 1723, 1743	CaAl ₂ Si ₂ O ₈ , Al ₆ Si ₂ O ₁₃ , SiO ₂
3	15.6	36.5	47.9	1785	298, 1873, 1913	CaAl ₂ Si ₂ O ₈ , Al ₆ Si ₂ O ₁₃ , Al ₂ O ₃

cooling to room temperature. The obtained specimens were glassy. Prior to exposure, the oxide powders Al₂O₃ and SiO₂ were ball-milled down to 3 µm particle size in the planetary ball mill Retsch PM 400 using the WC milling bodies. The particle size was controlled using the laser analyser Microsizer 201 A. The milled samples were subsequently melted in a molybdenum crucible. The congealed specimens were extracted from the crucible by drilling, using a diamond drill. The diameter of the drill was 10 mm less than the internal diameter of the crucible, so that the crucible walls were not hit by the drill. The extracted material was again ball-milled using the set-up mentioned above. The obtained milled powder was additionally purified using a laboratory scale magnetic separator. The traces of molybdenum were detected mostly close the specimen-crucible interface. The EDX analysis showed the bulk concentration of molybdenum in the specimen did not exceed 0.2 wt. %. After 3 h annealing of the extracted and milled powder in argon at 1500 °C, no traces of molybdenum oxide were detected by XRD. (X-ray diffraction) The same applies to tungsten and its oxides and carbides. The total concentration of impurities did not exceed 1 wt. %.

The powder samples were placed in a molybdenum crucible the inner surface of which was thoroughly ground and polished to minimise the



Figure 1. Sample 1 in molybdenum crucible after remelting

interaction between the melt and the crucible. The crucible was installed in the hot stage of the high-temperature diffractometer specially designed for studies on liquid melts [7-8]. Such set-ups, originally developed in Russia and Japan, are described in detail elsewhere [1,9]. Fig. 1 shows sample 1 in the molybdenum crucible after re-melting.

The test temperatures given in Table 1 are above the melting points of the mentioned compositions and are shown in the CaO-Al₂O₃-SiO₂ phase diagram in Fig. 2 [6]. The test temperatures were gradually increased to ensure the homogeneity of the melt specimens, as some of the obtained intensity curves were not typical for a homogeneous melt sample. Table 1 contains the literature data for the CaO-Al₂O₃-SiO₂ samples investigated in the present study, as well as the newly determined phase compositions which agree with the CaO-Al₂O₃-SiO₂ phase diagram [6].

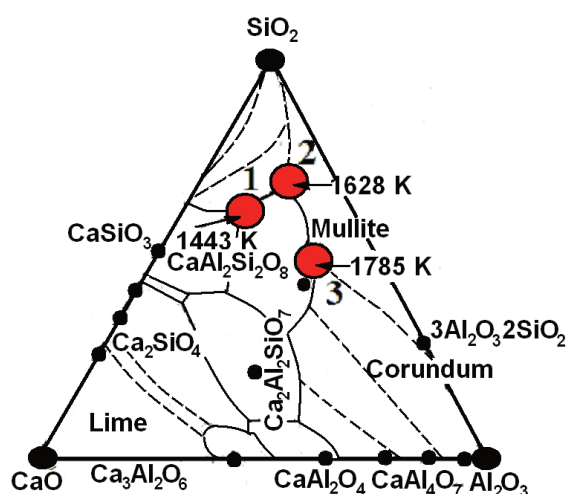


Figure 2. Phase diagram of CaO-Al₂O₃-SiO₂ system [6]; red circles mark the studied compositions

3. Results

3.1. Atomic distribution curves: melt structure

The experiments were conducted on the high-temperature θ - θ X-ray diffractometer using monochromatic MoK α radiation in a vacuum chamber filled with high purity helium. The experimental scattering intensity curves (IC) were obtained at temperatures specified in Table 1. The structure factor (SF) as well as the radial distribution function of atoms (RDF) were calculated using the program packages previously developed by the authors [7-8]. The experimental data were analysed using the Reverse Monte Carlo (RMC) method [7] to generate structural melt models. The calculation procedure is described in detail elsewhere [10-12].

Currently, the available experimental data on the CaO-Al₂O₃-SiO₂ are incomplete [13]. The melt

density values at the test temperatures (Table 1) are generally required for determination of the RDF curves and for the RMC method. The densities were estimated using the approach proposed in Ref [13]. This method is based on the analysis of the first pre-peak range on the RDF curve. It allows to obtain reasonable density values of the investigated melts.

Fig. 3 displays the SF and RDF curves for all three studied samples. The dotted lines in Fig. 3 are the SF curves retrieved from the RMC procedure which are in reasonable agreement with the experiment. The shape of the obtained SF curves is not typical for melts. The SF as well as the RDF curves obtained at lower temperatures substantially differ from those at higher temperatures. Additionally, the SF curves for sample 3 obtained at 1873 and 1913 K are virtually identical.

At lower temperatures, for some of the SF curves, the first peak may be smaller than the second one not exceeding unity. Above the melting point, the first SF peak is expected to be relatively high and usually exceeds unity. In our previous studies [7-8], such phenomena were observed at temperatures very close to the melting point. These effects are associated with incomplete melting of the liquid in which crystal-like aggregates are present. This phenomenon is known in the literature as the after melt effect [7-8]. It should be mentioned that liquid ordering does not prevail in this case and leads to such an unusual shape of the experimental IC and SF curves. Therefore, structural studies on the melts are generally conducted at temperature 50-100 K above the melting point. It is well known that above the melting point the atomic rearrangements become less pronounced with increasing temperature. The intensity of the first IC and SF peaks slightly decreases with the parallel broadening of the peak, which is related to disordering of the melt with increasing temperature. In the present case, the opposite is observed - the intensity of the first peak on the IC and SF (Fig.3.1) intensifies with increasing temperature for all three studied melt samples. Although the SF curves for sample 3 are very similar at the elevated temperatures, the first SF peak is also slightly higher at 1913 K compared to that at 1873 K (Fig. 3.1c). The observed anomalous temperature dependence of the first SF peaks is most likely related to the peculiarities of the melt structure of the studied samples. It may mean that the local atomic ordering in these melts enhances when the temperature is increased.

Although the experimental SF curves reveal no clear trend, the RDF curves for all three samples are quite similar. The similarities are observed in the range of the first and the second peaks which are usually considered in structural studies. The first peak on the RDF curve corresponds to the contribution of the Si-O and Al-O coordination to the atomic distribution [8]. This enables the determination of the closest

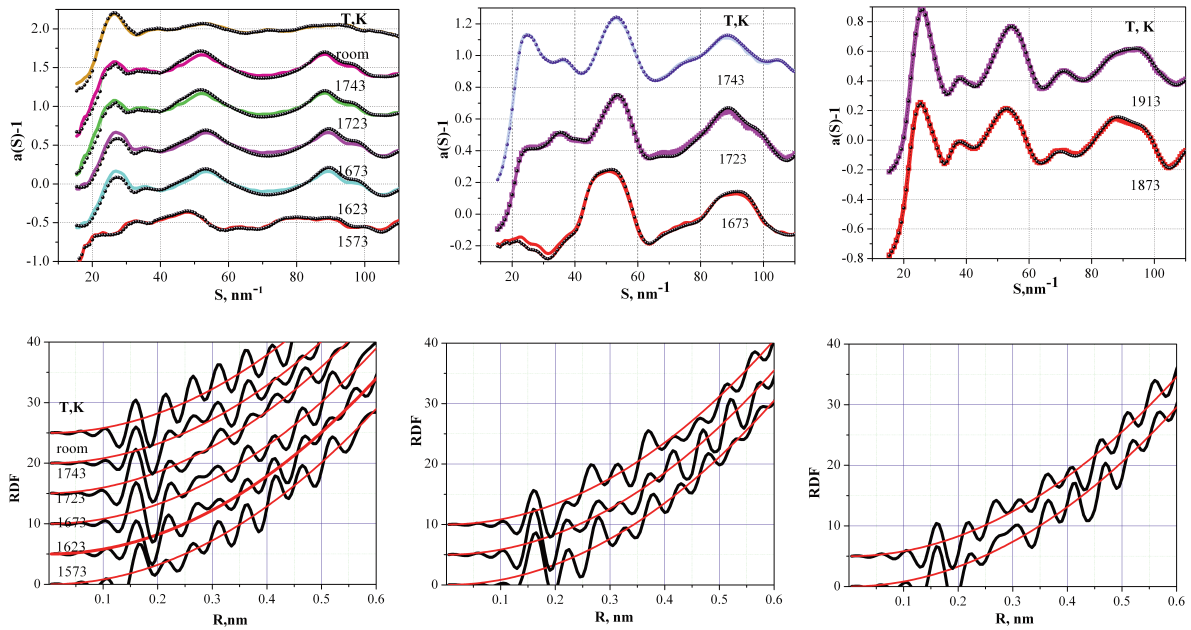


Figure 3. Structure factor (1) and atomic distribution (2) curves for studied slag melts of the $\text{CaO-Al}_2\text{O}_3\text{-SiO}_2$ system: (a) – sample 1, (b) – sample 2, (c) – sample 3

interatomic spacing $r_{\text{Al-O}}$, $r_{\text{Si-O}}$ and the coordination numbers for silicon and aluminium atoms with respect to oxygen $Z_{\text{Si-O}}$ and $Z_{\text{Al-O}}$, respectively. In a similar manner, the second RDF peak corresponds to the contribution of the Ca-O coordination [7-8]. The calculated values of the structural parameters are summarised in Table 2 along with the calculated melt densities (ρ), the positions of the first and the second SF peaks, S_1 and S_2 , respectively, and the surface areas below the first (Q_1) and the second (Q_2) peaks on the RDF curves. Interestingly, the coordination number for aluminium $Z_{\text{Al-O}}$ varies from 4.1 to 5.3, i.e. the aluminium atoms assume octahedral and partially tetrahedral positions in the oxygen framework. In sample 1, mostly the tetrahedral positions are

occupied, while in the other two samples the occupation of the octahedral positions is observed; this was to be expected because of the increasing concentration of alumina in melts. The latter effect intensifies with increasing temperature.

Surprisingly, the $Z_{\text{Ca-O}}$ values seem to be overestimated. In the previously studies slag melts, $Z_{\text{Ca-O}}$ values were close to 6, which suggested a slag melt model based on the close-packed spherical microassociates in a disordered liquid matrix [7-8]. The microassociates are in diffuse equilibrium with the liquid matrix. The microassociates are based on the spherical close-packed oxygen framework. The tetrahedral and octahedral voids of the framework are filled with atoms of different size. Smaller atoms are

Table 2. Structural parameters of studied slag melt samples

Options №	T, K	ρ , g/cm ³	S_1 , nm ⁻¹	S_2 , nm ⁻¹	r_1 , nm	Q_1	r_2 , nm	Q_2	$Z_{\text{Al-O}}$, Atom	$Z_{\text{Ca-O}}$, atom
1	2	3	4	5	6	7	8	9	10	11
1	298	2.9	27.2	53.3	0.16	1.73	0.217	1.31	4.1	8.9
	1573	2.8	22	47	0.162	1.77	0.219	1.85	4.3	7.7
	1623	2.8	26.6	52.2	0.161	1.8	0.221	1.87	4.5	11.6
	1673	2.7	26.9	53.3	0.161	1.87	0.224	1.73	4.8	11.8
	1723	2.7	26.3	53	0.161	1.83	0.224	1.74	4.5	9.6
	1743	2.6	27.1	53.3	0.16	1.75	0.223	1.75	4.1	9.6
2	298	3	24.8	53.2	0.162	2.3	2.221	0.92	5.2	9.9
	1673 1723	2.8	-	51.4	0.164	2.38	0.223	1	4.4	11
	1743									
		2.8	25.2	53.3	0.163	2.36	0.222	0.89	4.8	9.8
		2.8	24.9	53.3	0.163	2.31	0.222	0.95	5.3	10.4
3	298 1873	3	25.4	54.3	0.163	2.34	0.223	1.3	5.1	9.4
	1913	2.6	25.1	52.3	0.162	2.31	0.224	1.42	4.9	10.8
		2.6	25.3	54.5	0.161	2.35	0.222	1.19	5.1	9.1

localized in the tetrahedral voids closer to the microassociate core. In the intermediate layer, both the tetrahedral and octahedral voids are partially occupied by the atoms of medium size. The largest atoms occupy exclusively the octahedral voids in the outer part of the microassociate. In such melts, increasing temperature results in a dissociation of the outer layer containing larger cations. Further temperature increase may destruct the core, thus transforming the system into a homogeneous melt.

In the present study, the $Z(\text{Ca-O})$ values vary from 7.7 to 11.8. Thus, the calcium cations cannot occupy the octahedral voids in the oxygen framework. Presumably, the octahedral and tetrahedral voids of the oxygen framework are filled with the silicon and aluminium cations while the larger calcium ions are located outside the oxygen framework and are weakly bonded with it. The oxygen environment of the calcium ions consists of the surface oxygen atoms of the microaggregates and the oxygen atoms from the liquid medium around the core. Thus, the calcium cations form the outer diffusive layer around the microparticles [15] and neutralize the negative surface charge of the oxygen framework surrounding the microaggregates.

Fig. 4 shows the experimental IC's for sample 1 at 1673 K and sample 3 at 1913 K. Fig. 4b contains powder diffractogram for crystalline mullite. The comparison between the experimental diffractogram (1) and the standard mullite XRD pattern (2) allows concluding that the experimental one contains weak mullites peaks. Weaker mullite peaks were also found in the diffractogram of sample 2. The XRD patterns of the as-quenched samples at room temperature are very similar to the XRD patterns of the melts. These findings suggest the formation of the mullite Al-Si-O micro-aggregates during melting. The weak intensity of these peaks [17] is related to an extremely small size of the aggregates.

The calculated IC (Fig.4a) was obtained by summarizing XRD of the blurred mullite crystal cell

and "melt" background using the PowderCell software. It should be noted that experimental and calculated IC's are in good agreement.

The calculations for sample 1 performed using the PowderCell program predicted the region of coherent scattering for mullite to be 8.0-8.5 nm, 30-37 nm for CaSiO_3 and 32 nm for SiO_2 . According to Ref [17], the intensity of crystalline peak may hardly exceed the background when the crystallites are smaller than 20 nm.

3.2. Structural models for melts based on RMC

The RMC calculations were carried out using the standard open source program RMC-3-14. The initial configuration consists of randomly set 5000 atoms in a stoichiometric proportion. The atoms are placed in a basic cell with a periodic boundary condition [10, 11]. The program has the following algorithm. A given displacement of a random atom is performed in the system. The SF curve is calculated for the new configuration and is compared versus the experimental curve. If the displacement improves the agreement between the experimental and predicted SF curves, the displacement is accepted. In the opposite case, the iteration step is rejected. The optimization procedure is carried on until an acceptable agreement within the experimental error between the experimental and predicted SF curves is achieved. Such a procedure usually requires some millions of iterations. The optimization results in a structural model of the studied melt yielding the best-fit spatial distribution of atoms, as well as the quantitative parameters of the surrounding atom environments.

For example, Fig. 5 shows the partial pair distribution curves of atoms $g_{i,j}(r)$, as well as the coordination number distribution for sample 1 at room temperature. Virtually identical curves were obtained for the other samples at different temperatures. The $g_{ij}(r)$ curves for the Si-O, Al-O and Ca-O coordination types are presented in Fig. 5 (1a, 2a and 3a) while the

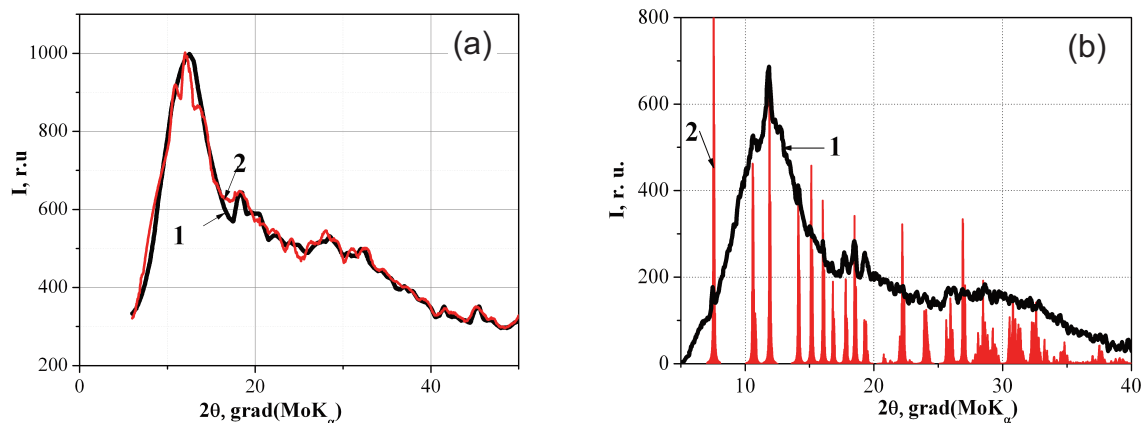


Figure 4. The experimental IC's (1) for sample 1 at 1673 K (a) and sample 3 at 1913 K (b), the reflexes (2) of crystalline mullite are shown in Fig. b, calculated IC (2) assuming the blurred mullite crystal cell is shown in Fig. a

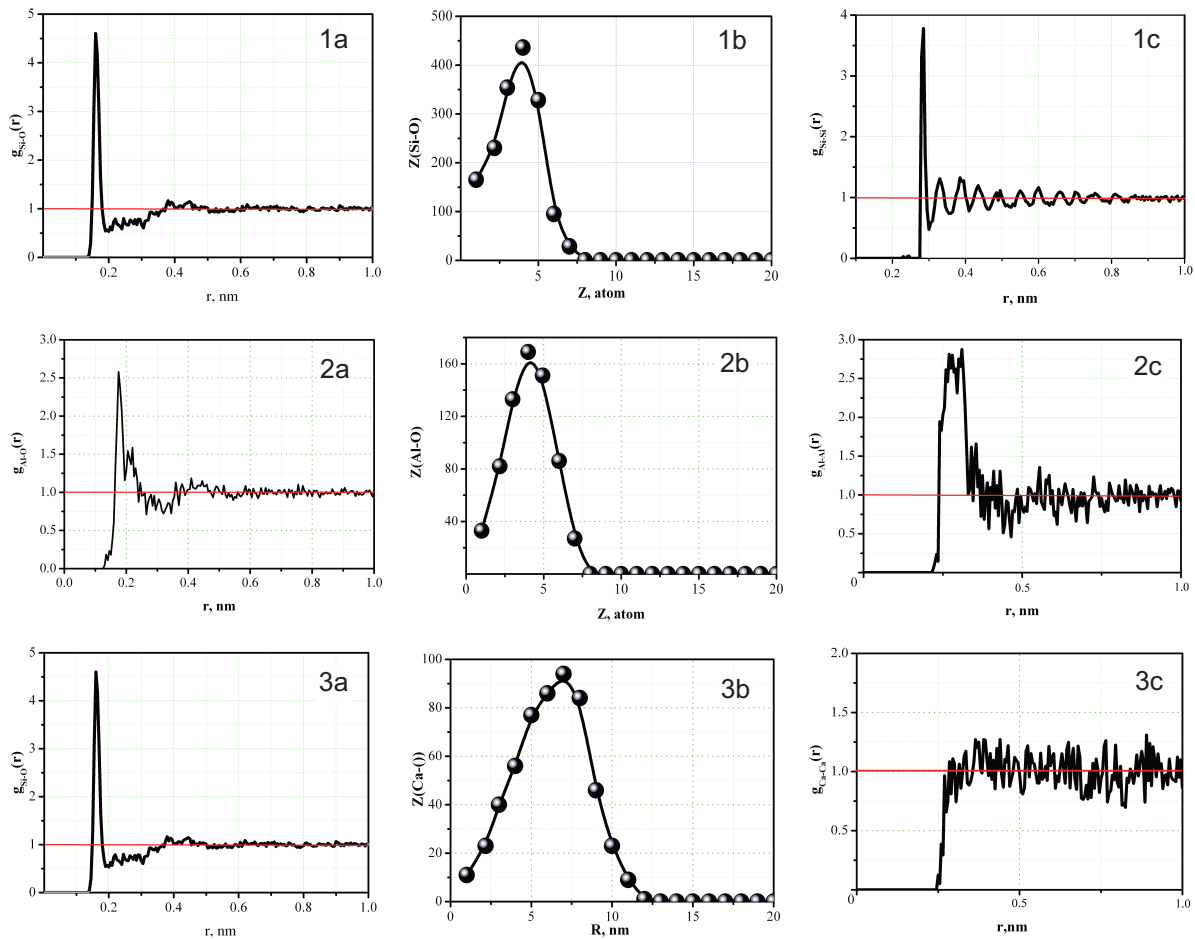


Figure 5. Partial $g_{ij}(r)$ curves (a) and coordination number distribution (b) for Si-O (1), Al-O (2) and Ca-O (3) coordination and $g_{ij}(r)$ curves (c) for Si-Si (1), Al-Al (2) and Ca-Ca coordination for sample 1

corresponding coordination number ($Z_{(Si-O)}$, $Z_{(Al-O)}$ and $Z_{(Ca-O)}$) distribution curves are shown in Fig. 5 (1b, 2b and 3b). The calculated interatomic spacing values, as well as the most probable coordination number values, agree well with those obtained from the RDF analysis.

The calculated $r_{1(Si-O)}$ values for all samples and temperatures is 0.165 ± 0.003 nm. The coordination number $Z_{(Si-O)}$ is calculated to be 4 ± 0.3 , which implies that the tetrahedral oxygen environment for silicon is maintained at all test temperatures. In the same manner, the Al-O spacing was calculated from the $g_{Al-O}(r)$ curve to be 0.181 ± 0.003 nm, while the coordination number maximum is located around 4. The coordination number distribution is asymmetric shifted towards the higher r values. The spacing $r_{1(Ca-O)}$ for all compositions was calculated to be 0.223 ± 0.005 nm, $Z_{(Ca-O)}$ varies from 7.7 to 11.8. For all temperatures and compositions, the partial pair distribution curves for the Si-Si coordination (Fig. 5,c1) have an unusual shape, i.e. several alternating peaks, which is rather typical for a crystalline specimen. The clear first peak on the $g_{Al-Al}(r)$ curve (Fig.5,c2) implies that the correlation in the

distribution of aluminium atoms is limited mainly to the closest neighborhood. At the same time, the shape of the $g_{Ca-Ca}(r)$ curve (Fig.5, c3) is indicative of a random distribution of calcium atoms.

4. Discussion

The obtained results based on the standard analysis of the experimental data, as well as those generated through the RMC procedure, are reasonable and in good agreement. However, their interpretation is difficult for a number of reasons. Several experimental facts such as low intensity of the first peak on the SF curve, strong temperature dependence of the SF curves, an unusual shape of the $g_{Si-Si}(r)$ and $g_{Al-Al}(r)$ curves, suggest that the experimental IC and SF curves, as well as the calculated ones, exhibit untypical features for melts.

Weak peaks of mullite and/or sillimanite on the IC (the similar diffractograms of both modifications are shown in Fig. 6a) are observed for the initial samples at room temperature, as well as above the melting point.

These two crystal modifications have similar

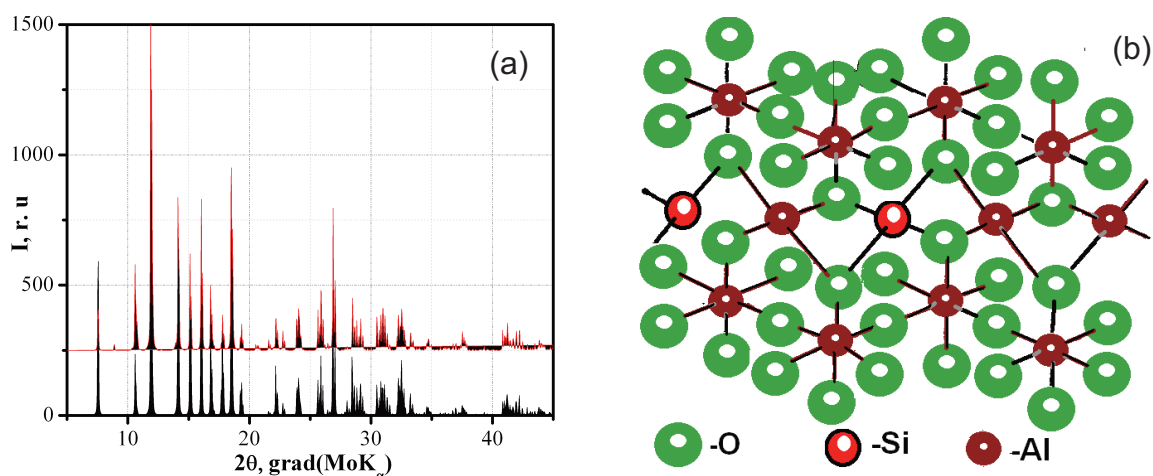


Figure 6. (a) – mullite (black) and sillimanite (red) diffractograms; (b) – ideal mullite cell

structural types of Pbam for mullite and Pbnm for sillimanite. Importantly, the *c* parameter of the mullite cell is smaller by a factor of 2 than that for sillimanite. The other cell parameters are quite similar. Thus, a precise determination of the ordering type in the microaggregates is impossible in the present study. The ideal mullite cell is shown in Fig. 6b [16,17]. The extremely high $Z_{(Ca-O)}$ values indicate that calcium does not play a role in the formation of the microaggregates in the melt.

It is worth mentioning that the partial $g_{i-j}(r)$ curves retain their shape even if the SF and RDF curves strongly change. The short-order parameters for the Si-O and Al-O coordination bonds also remain unchanged, being close to the characteristic values previously obtained or present in the literature on silicate melts.

The features above might be interpreted in the following manner. The peculiarities of the diffraction data obtained in the given temperature interval should be attributed to a heterogeneous microstructure of the melt containing microparticles. The liquid constituent of the melt is a disordered matrix. The chaotically distributed aluminosilicate microparticles are in a diffuse equilibrium with the liquid disordered matrix. The calcium cations are located on the surface of the aluminosilicate microcrystallites partially compensating for a negative surface charge of the oxygen ions of the crystallite. The oxygen ions in the disordered matrix neutralise the slight excessive positive charge of the calcium cations in turn. Thus, a core of a microparticle consisting of a mullite-sillimanite microcrystallite surrounded by the calcium ions can be assumed. The core is further surrounded by the oxygen ions from the disordered matrix, thus forming a diffuse layer around the aggregate. The microparticles intensively interact with the liquid disordered matrix. Presumably, the microaggregate is an aluminosilicate of the mullite and/or sillimanite type.

The type of the microaggregate is difficult to predict as its structure is composition and temperature dependent.

Sillimanite was previously reported [6] to decompose at approx. 1823 K forming mullite per equation (1)

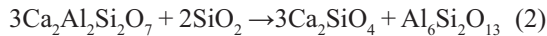


One should not rule out a possibility of continuous transformation depending on the composition and the temperature. Mullite is preferable at higher temperatures, while several samples tested at lower temperatures may contain sillimanite. However, it should be noted that the peak on the $g_{Si-Si}(r)$ (see Fig. 5c1) does not correspond to the closest Si-Si spacing either for mullite or for sillimanite.

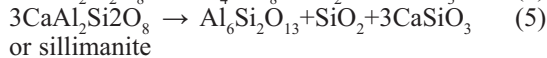
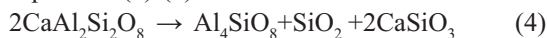
The formation of mullite-sillimanite microaggregates does not depend on larger calcium cations. These cations are located at the interface between the ordered microparticle and the disordered slag matrix, partially neutralizing the negative charge of the surface of the oxygen scaffold. The calcium cations are weakly bound to the microcrystallite, surrounded by oxygen ions from the matrix of molten slag. This structure reduces the interaction between calcium ions and the anionic medium, which leads to high values of $Z(Ca-O)$.

The temperature dependence of the SF curves (e.g. increasing intensity of the first peak with increasing temperature) might be related either to the compositional changes in both solid and liquid phases or to a higher ordering degree of the liquid phase. Crystallites smaller than 10 nm are characterized by much lower X-ray reflectivity compared to bulk (the size > 20 nm) powder KI [17]. Such reflexes are hardly distinguishable from the background. Since our experience with heterogeneous liquid-solid system is rather limited, further effects may play a role in the systems under investigation. However, it was established that the magnitude of the first peak is not always the highest at the liquidus temperature. In our experiments, the specimens are usually heated to the temperature which is 50-100 K above the melting point. At this point, the magnitude of the first peak

and the further ones can be reasonably calibrated. The SF values oscillate around unity, slowly decaying. Thus, our experiments were conducted not in a fully molten slag, but in a heterogeneous range with the aluminosilicate microcrystallites immersed in the liquid melt. Are the mullite-sillimanite microcrystallites real? The mullite formation reaction was assumed in Ref [5]:



where the formed aluminosilicate is mullite, the composition ranging from Al_4SiO_8 to $\text{Al}_6\text{Si}_2\text{O}_{13}$. In the present study, the composition of the samples lays in the anorthite $\text{CaAl}_2\text{Si}_2\text{O}_8$ range. At higher temperatures, anorthite decomposes forming mullite pre equations (4)-(5)



or sillimanite



It should be noted that in contrary to the phase diagram $\text{CaO-Al}_2\text{O}_3\text{-SiO}_2$ there is experimental data about non-congruent melting of the anorthite Ref [6, 18].

The mullite formation was corroborated by an additional exposure after 1h of annealing at 1373 K of sample 1. The XRD patterns of this sample were refined using the PowderCell software. Three phases were detected in the sample: silica, wollastonite and mullite although the mullite formation is rather the least probable. Fig. 7 demonstrates the experimental diffractogram along with the calculated XRD pattern for a mixture $\text{SiO}_2 + \text{CaSiO}_3 + \text{mullite}$ (sillimanite). The individual diffractograms for silica, wollastonite and mullite are shown in the lower part of Fig. 7. In this sample, mullite may form by reactions (4) and (5), sillimanite by reaction (6).

Most likely, mullite forms from the anorthite decomposition reaction. However, it might have already existed prior to annealing at 1373 K. In samples 2 and 3, mullite can exist prior to reaction, its concentration increasing due to anorthite decomposition, since mullite is the reaction product. After the decomposition, the mullite (sillimanite) content in the sample is additionally increased by the excess of alumina and especially silica in the liquid phase.

It was mentioned in Ref [19] that the mullite structure is close to that of sillimanite, the fundamental difference being a peculiar statistic distribution of the silicon and aluminium atoms in the new tetrahedral sites which remain unoccupied in sillimanite. Since the diffractograms of both modifications are very similar, the formation of an oxide mullite-sillimanite framework may be tentatively assumed, the silicon and aluminium atoms statistically diffusing between the voids in this framework. Both the silicon to aluminium ratio in the

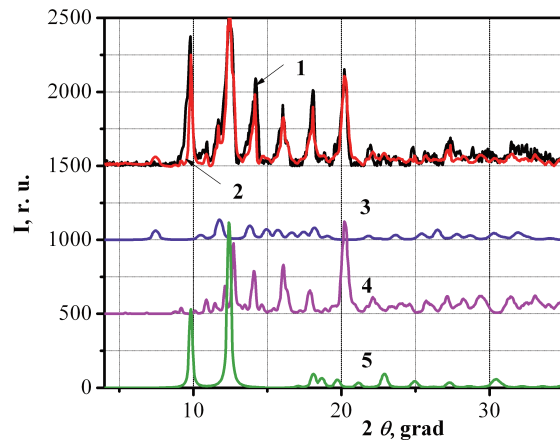


Figure 7. XRD pattern for sample 1 after 1 h at 1373 K (background subtracted) (1) and calculated with PowderCell integral diffractogram for $\text{SiO}_2\text{-CaSiO}_3\text{-mullite}$ mixture (2), along with the individual diffractograms for individual components: mullite (3), CaSiO_3 (4), SiO_2 (5)

tetrahedral voids $N_{\text{Si}(4)}/N_{\text{Al}(4)}$, and the tetrahedral to octahedral ration for the aluminium atoms $N_{\text{Al}(4)}/N_{\text{Al}(6)}$ are composition and temperature dependent. As this is our first study of a heterogeneous system, some conclusions might be debatable.

5. Conclusions

Silicon and aluminium are tetrahedrally coordinated by oxygen in the studied slag melt. However, a small fraction of aluminium silicon atoms forms oxygen octahedrons. The interatomic spacing values for the Si-Si and Al-Al bonds in the melts are in good agreement with the literature data for crystals and other molten oxide systems. The closest environment around the calcium ion Ca^{2+} consists of oxygen atoms, the interatomic spacing being 0.22-0.23 nm. The coordination number for calcium varies from 7.7 to 11.8.

The interatomic interaction as well as the atom distribution in the considered system cannot be viewed as solely liquid disordered structure. In our opinion, a heterogeneous mixture consisting of aluminosilicate microcrystallites immersed in a molten oxide matrix exists in the molten slag of the studied compositions at higher temperatures.

A model was proposed to describe the structure of such liquids which contain microaggregates. The aggregate consisting of the oxygen framework contains silicon and aluminium atoms forming a microcrystallite of the mullite-sillimanite type in the core.

The tetrahedral voids of the oxygen framework are filled with the silicon and partially with aluminium cations. A negligible fraction of the octagonal voids is occupied exclusively by the aluminium ions. The calcium cations are surrounded in turn by the surface oxygen of

the framework, thus constructing the core. The oxygen of the molten slag matrix along with the oxygen of the microaggregate framework form the closest environment of the calcium ions building up the particle.

The three phases (mullite, silicon dioxide and CaSiO_3) were detected in the fused sample No.1 at room temperature. These phases are also observed in the XRD patterns of the solid sample No.1 at 1373 K. The weak reflections of the mullite can be only identified in the XRD patterns of the melted sample up to 1723 K. This confirms the assumption of the stability of the phase based on mullite.

Since the XRD patterns of mullite and sillimanite are quite similar, none of them can be preferred when interpreting the diffraction results. However, mullite might be preferable, as it is known to be stable at higher temperatures.

References

- [1] V. Sokol'skii, A. Roik, A. Davidenko, V. Kazimirov, V. Lisniak, V. Galinich, I. Goncharov, J. Min. Metall. Sect. B-Metall., 48 (1) B (2010) 101-113.
- [2] M. Kumar S.Sankaranarayanan, J. Min. Metall. Sect. B-Metall., 44 (1) B (2008) 133-135.
- [3] F. Kongoli, I. McBow, R. Budd, S. Llubani, A. Yazawa, J. Min. Metall. Sect. B-Metall., 46 (2) B (2010) 123-130.
- [4] E. Pastukhov, N.Vatolin, V.Lisin. et al. Diffraction studies of a structure of high-temperature melts. Ur. Div. Rus. Acad. Sci. Ekaterinburg., 2003. p.544.
- [5] N. Vatolin, E. Kern, V. Lisin, X-Ray study of silicate melts. Chapter 1 in Structure and physical-chemical properties of metallic and oxide melts. UNC AS USSR, Sverdlovsk, 1986, p. 38-56.
- [6] A. Berezhnoy, Multicomponent oxide systems, Naukova dumka, Kiev, 1970, p. 542
- [7] V. Sokol'skii, O. Roik, V. Kazimirov et al., Practical Application of X-Ray Analysis to the study of Welding Fluxes at High Temperature., Chapter 5, In Advances in Materials Science Research. V20.: Nova Science Publishers, NY, 2015, p.95-128.
- [8] V. Sokol'skii, V. Kazimirov, V. Lisnyak et al, Welding Fluxes: Structural and physicochemical aspects of slag melts. PPC "The University of Kyiv", Kiev, 2015 p. 240.
- [9] Y. Waseda., J. Toguri, The Structure and Properties of Oxide Melts: Application of Basic Science to Metallurgical Processing, World Scientific, Singapore, 1998. p.217.
- [10] R. McGreevy, J. Phys.:Condens. Matter, 13 (46) (2001) R877-R913.
- [11] A. Le Ball, J. Non-Cryst. Solids.; 271, (2000) 249–259.
- [12] D. Keen, R. McGreevy, Nature, 344, (1990) 423–425.
- [13] M. Allibert, H. Gaye, et al Slag Atlas. Verlag Stahleisen M.B.H, Dusseldorf, 1995, p.365.
- [14] A. Il'inski, A. Romanova, L. Mikhailova et al, Metallofizika, Kiev, 13 (2), (1991); 119–122.
- [15] S. Voiutski, The course of colloid chemistry, Chemistry, Moscow, 1964. p.461.
- [16] Yu. Putilin, Yu. Beliakova, V. Holenko et al , Synthesis of minerals V. 2, Nedra, Moscow, 1987. p. 218.
- [17] L. Kheiker., D. Zevin, X-Ray diffractometry Fizmatiz, Moscow, 1963. p.230.
- [18] A. Berezhnoy, Multicomponent alkali oxide systems, Naukova dumka, Kiev 1988. p.458.
- [19] S. Diurovich, J. Amer. Ceram. Soc. 45, (1962), 157-161.

ISPITIVANJE STRUKTURE RASTOPLJENIH $\text{CaO-Al}_2\text{O}_3\text{-SiO}_2$ KAO OSNOVE ZA RAZVOJ NOVIH AGLOMERISANIH FLUKSEVA ZA ZAVARIVANJE I INDUSTRIJSKIH VATROSTALNIH MATERIJALA

V.E. Sokol'skii^a, D.V. Pruttskov^b, V.M. Busko^b, V.P. Kazimirov^a, O.S. Roik^a, A.D. Chyrkin^a,
V.I. Galinich^c, I.A. Goncharov^c

^a Nacionalni univerzitet Kijeva Taras Ševčenko, Kijev, Ukrajina

^b ZAO Tehnokim, Zaporozhje, Ukrajina

^c E.O.Paton Institut za električno zavarivanje

Apstrakt

U Ukrajini postoji značajna proizvodnja flukseva za zavarivanje i industrijske keramike. Proizvodnja ovih materijala je dovoljna kako za domaće potrebe tako i za značajan izvoz. Pretpostavlja se da bi ternarni $\text{CaO-Al}_2\text{O}_3\text{-SiO}_2$ sistem mogao da postane osnova za razvoj aglomerisanih flukseva za zavarivanje i tehničke keramike. Tri uzorka ternarnog $\text{CaO-Al}_2\text{O}_3\text{-SiO}_2$ sistema je ispitivano uz pomoć visokotemperaturne rentgenske difrakcije iznad tačke topljenja: 23.3CaO-14.7Al₂O₃-62.0SiO₂ wt. % (uzorak 1, eutektičan), 9.8CaO-19.8Al₂O₃-70.4SiO₂ wt. % (uzorak 2, eutektičan), 15.6 CaO-36.5Al₂O₃-47.9SiO₂ wt. % (uzorak 3). Dobijeni su eksperimentalni intenziteti kriva rasipanja, strukturni faktori i radijalna funkcija atoma. Izračunati su strukturalni parametri kratkog raspona korišćenjem modela strukture topljenja dobijenog Reverse Monte Carlo metodom. Pretpostavlja se postojanje mikročestica tipa mulita ili sillimanita uronjenih u matricu šljake. Pretpostavlja se da su joni kalcijuma koordinisani oko ovih čestica okruženi anjonima kiseonika otopljenih metala. Ovakva struktura može se smatrati koloidalnim rastvorom. Mikročestice mulita su jezgro agregata okruženog jonima kalcijuma i kiseonika iz otopljenog materijala

Ključne reči: Rastopljeno stanje; Heterogene oblasti; Mulit; Eutektični; Rentgenska metoda; Struktura

